Fabrication and ultraviolet detection performance of ZnO NRs/Porous GaN heterojunction

YANG Xu-dong, JIA Wei, XIAO Yan-qing, WANG Xia-long, LI Tian-bao, ZHAI Guang-mei, DONG Hai-liang, XU Bing-she

Citation:
YANG Xu-dong, JIA Wei, XIAO Yan-qing, WANG Xia-long, LI Tian-bao, ZHAI Guang-mei, DONG Hai-liang, XU Bing-she. Fabrication and ultraviolet detection performance of ZnO NRs/Porous GaN heterojunction[J]. *Chinese Optics*, In press. doi: 10.37188/CO.EN-2026-0016
杨旭东, 贾伟, 肖燕青, 王夏龙, 李天保, 翟光美, 董海亮, 许并社. ZnO纳米棒/多孔GaN异质结的制备及紫外探测性能研究[J]. 中国光学, 优先发表. doi: 10.37188/CO.EN-2026-0016

View online: https://doi.org/10.37188/CO.EN-2026-0016

文章编号　2097-1842(xxxx)x-0001-15

Fabrication and ultraviolet detection performance of ZnO NRs/Porous GaN heterojunction

YANG Xu-dong[1], JIA Wei[1 *], XIAO Yan-qing[3], WANG Xia-long[1], LI Tian-bao[1], ZHAI Guang-mei[1], DONG Hai-liang[1], XU Bing-she[1,2]

(1. *Key Laboratory of Interface Science and Engineering in Advanced Materials*, *Taiyuan University of Technology*, *Taiyuan*, 030024, *China*;
2. *Institute of Atomic and Molecular Science*, *Shanxi University of Science and Technology*, *Xi'an*, 710021, *China*;
3. *Shanxi Dingxin Crystal Materials Co.*, *Ltd*, *Taiyuan*, 030032, *China*)

* *Corresponding author*, *E-mail*: *jiawei@tyut.edu.cn*

Abstract: Owing to the limited interfacial contact area, insufficient carrier transport efficiency, and the adverse effects of intrinsic defects in ZnO on photoresponse, further improvement in the performance of conventional ZnO/GaN heterojunction ultraviolet photodetectors remains restricted. To address these issues, Ga+Al co-doped ZnO nanorod arrays with different Ga doping concentrations were grown on porous p-GaN/Al_2O_3 substrates by a low-temperature hydrothermal method, and the corresponding Ga+Al co-doped ZnO nanorod/porous GaN heterojunctions were fabricated. The porous p-GaN structure was used to enhance heterojunction interfacial contact and light absorption, while Ga+Al co-doping was employed to regulate the defect states and carrier transport properties of ZnO nanorods, thereby improving the self-powered ultraviolet photodetection performance of the devices. The findings of the study demonstrated that under 365 nm ultraviolet illumination at 0 V bias, the device with a Ga doping concentration of 3 at.% exhibited the best UV photodetection performance, with a light/dark current ratio of 8250, a responsivity (R) of 0.158 A/W, a specific detectivity (D^*) of 3.15×10^{12} Jones, and an external quantum efficiency (EQE) of 53.5%. This study provides useful theoretical insight and experimental support for the development of next-generation high-performance ZnO/GaN-based heterojunction ultraviolet photodetectors.

Key words: porous GaN; low-temperature hydrothermal method; ZnO nanorods; ZnO nanorod/GaN heterojunction; ultraviolet photodetector

收稿日期:2026-05-19; **修订日期:**2026-05-28
基金项目:山西省重点研发计划项目 (No.202502030202046)
Key R&D Program of Shanxi Province (No.202502030202046)

ZnO 纳米棒/多孔 GaN 异质结的制备及紫外探测性能研究

杨旭东[1], 贾　伟[1*], 肖燕青[3], 王夏龙[1], 李天保[1], 翟光美[1], 董海亮[1], 许并社[1,2]
（1. 太原理工大学新材料界面科学与工程教育部重点实验室, 山西太原 030024;
2. 陕西科技大学原子与分子科学研究所, 陕西西安 710021;
3. 山西鼎芯晶体材料有限公司, 山西太原 030032）

摘要: 由于传统 ZnO/GaN 异质结紫外光电探测器仍存在界面接触面积有限、载流子输运效率不足以及 ZnO 本征缺陷影响光电响应的问题, 限制了器件性能的进一步提升。因此本文采用低温水热法在多孔 p-GaN/Al_2O_3 衬底上生长了不同 Ga 掺杂浓度的 Ga+Al 共掺杂 ZnO 纳米棒阵列, 并制备了相应的 Ga+Al 共掺杂 ZnO 纳米棒/多孔 GaN 异质结, 通过多孔 p-GaN 增强异质结界面接触与光吸收, 并利用 Ga+Al 共掺杂调控 ZnO 纳米棒的缺陷状态和载流子输运性能, 从而提高器件的自供电紫外探测性能。结果表明, 在 0 V 偏压和 365 nm 紫外光照下, Ga 掺杂浓度为 3% 时器件表现出最佳的紫外探测性能, 其光暗电流比为 8250、响应度(*R*)为 0.158 A/W、比探测率(D^*)为 3.15×10^{12} Jones、外量子效率(*EQE*)为 53.5%。该研究为制备下一代高性能 ZnO/GaN 基异质结紫外光电探测器提供了一定的理论指导和实验数据。

关 键 词: 多孔 GaN; 低温水热法; ZnO 纳米棒; ZnO 纳米棒/GaN 异质结; 紫外光电探测器
中图分类号: TN248.4　**文献标志码:** A　**doi:** 10.37188/CO.EN-2026-0016　**CSTR:** 32171.14.CO.EN-2026-0016

1 Introduction

Ultraviolet photodetectors based on p-n junctions composed of wide-bandgap semiconductors offer the advantages of low dark current, high sensitivity, and good stability and therefore show broad application prospects in environmental monitoring, ultraviolet communication, and space exploration[1-4]. Gallium nitride (GaN), a typical wide-bandgap semiconductor, possesses high carrier mobility and excellent thermal stability, making it an attractive candidate for ultraviolet photodetectors[5]. In addition, porous GaN films, owing to their large specific surface area and enhanced light-harvesting capability, can effectively promote the generation and collection of photogenerated carriers, thereby further enhancing photodetection performance[6]. To date, various methods have been reported for the fabrication of porous p-GaN films, including electrochemical etching (EC)[7], ultraviolet-assisted electrochemical etching (UV-EC)[8], reactive ion etching (RIE)[9] and high-temperature annealing (HTA)[10]. Among these approaches, high-temperature annealing has attracted considerable attention because of its simple processing procedure, operational convenience, and the avoidance of electrolyte-derived impurity ions. Chen *et al.*[11] proposed a new method for fabricating porous GaN by high-temperature annealing in a nitrogen atmosphere. Compared with the as-grown sample, the porous GaN prepared at 1 050 °C exhibited higher carrier mobility, a faster photoresponse, and comparable visible-light transmittance. Meng *et al.*[12] reported a Ga_2O_3/nanoporous GaN MIS photodetector fabricated by thermal oxidation, which exhibited a responsivity as high as 4.5×10^5 A/W and a maximum external quantum efficiency of 1.55×10^8%. Yu *et al.*[13] investigated the effects of annealing temperature and duration on the pore size, density, and depth of porous GaN, achieved precise control over the porous structure and subsequently fabricated a high-performance porous n-GaN MSM photodetector with a dark current of 0.11 mA, an on/off ratio of 29.09, and a decay time of 1.553 s. Compared with MSM and MIS photodetectors, p-n junction photodetectors generally exhibit lower dark current, lower power consumption, and higher sensitivity[14,15]. Therefore, heterojunction devices based on p-GaN and various n-type semiconductors have become a major focus of research. Guo *et al.*[16] fabricated a porous GaN/CuZnS heterojunction near-ultraviolet photodetector that delivered a peak responsivity of 0.41 A/W, an external quantum efficiency of 138.6%, and a specific detectivity of 9.8×10^{12} Jones. Varshney *et al.*[17] fabricated a Ga_2O_3/GaN heterojunction ultraviolet photodetector via a simple thermal oxidation process. Under 266 nm illumination at a bias voltage of 5 V, the device exhibited a responsivity of 2.21×10^5 mA/W, an external quantum efficiency of 6.8×10^4%, and a specific detectivity of 7.71×10^{11} Jones. Nevertheless, the fabrication of ZnO/GaN heterojunction devices remains insufficiently mature, and their photodetection performance still requires further improvement. Therefore, further exploration of the fabrication and performance optimization of novel ZnO/GaN heterojunction devices remains of great importance.

Zinc oxide (ZnO), another typical wide-bandgap semiconductor, possesses excellent chemical stability and optoelectronic properties. With a bandgap of approximately 3.37 eV and a high exciton binding energy of up to 60 meV, ZnO has shown great potential for ultraviolet photodetection applications[18,19]. In particular, one-dimensional ZnO nanorod (NR) structures, owing to their large specific surface area, direct carrier-transport pathways, and short transport distances, can effectively enhance light harvesting and improve carrier transport efficiency, thereby providing favorable conditions for the fabrication of high-performance ultraviolet photodetectors[20]. In addition, both ZnO and GaN crystallize in the hexagonal wurtzite structure, and their similar bandgaps together with the small lattice mismatch facilitate the formation of high-quality heterojunction interfaces, thus providing a sound material basis for the fabrication of high-performance ultraviolet photodetectors[21]. Consequently, ZnO/GaN heterojunction photodetectors have attracted widespread attention. Kaur *et al.*[22] reported an n-ZnO/(0001) p-GaN heterojunction ultraviolet photodetector with a responsivity of 11 mA/W, a response time of 0.7 ns, and a minimum detectable optical power of 9 nW. Fan *et al.*[23] fabricated a self-powered ZnO-mesh/GaN heterojunction ultraviolet photodetector by chemical vapor deposition (CVD). Under 355 nm illumination at zero bias, the device achieved a voltage responsivity of 2200 V/W, and its response time was significantly reduced from 3.14 ms to 392 µs.

The stability of ZnO is strongly influenced by intrinsic point defects, such as oxygen vacancies (V_O) and zinc interstitials (Zn_i), which play crucial roles in determining the performance of ZnO-based optoelectronic devices[24]. To address this issue and improve the optoelectronic performance of ZnO films and nanostructures, extensive efforts have been devoted to donor doping in ZnO. Among the various dopants, group III elements such as Al, Ga, and In have attracted considerable attention because they can effectively improve the electrical and optical properties of ZnO nanostructures. Previous studies have shown that doping with Ga, Al, or In not only significantly improves the electrical conductivity of ZnO but also tunes its optical bandgap, thereby optimizing device performance[25]. On this basis, co-doping strategies have been further employed to tailor the properties of ZnO nanostructures through the synergistic incorporation of two group III elements, such as Al-Ga, Al-In, and Ga-In. Compared with single-element doping, co-doping generally provides higher carrier concentrations and thus improves the electrical conductivity of the material[26]. Tsay *et al.*[27] fabricated a heterojunction photodetector based on a p-GaN film and an n-type ZnO nanowire array. Their study revealed that, compared with undoped and singly doped devices, the Ga-In co-doped ZnO (GIZO) device exhibited superior photoresponse performance, achieving a light/dark current ratio of approximately 6.0 and a turn-on voltage of 1.77 V under ultraviolet illumination. Lung *et al.*[28] prepared Al-Ga co-doped ZnO films by radio-frequency magnetron sputtering. The results showed that the optical bandgap of the films changed markedly with increasing Al and Ga doping concentrations, reflecting an increase in carrier concentration. Therefore, constructing heterojunctions by integrating GaN with Ga+Al co-doped ZnO nanostructures is an effective strategy for enhancing ultraviolet photodetection performance.

In this work, porous p-GaN films were first prepared by N_2 and H_2 assisted high-temperature annealing, followed by the fabrication of ZnO nanorod/porous GaN heterojunctions on the porous GaN films via a low-temperature hydrothermal method. The crystal structure, optical absorption characteristics, and ultraviolet photodetection performance of the resulting heterojunctions were systematically investigated.

2 Experiment section

2.1 Preparation of porous p-GaN

The p-GaN epitaxial wafers used in this study were provided by Shanghai GaNova Electronic Information Co., Ltd. The epitaxial structure consisted of a 2.5-μm-thick unintentionally doped GaN layer and a 1-μm-thick Mg-doped p-GaN layer. Prior to the experiments, the p-GaN wafers were first cut into small pieces measuring 10 mm×5 mm to facilitate the subsequent growth of ZnO nanorod arrays. The GaN films were sequentially ultrasonically cleaned in acetone, ethanol, and deionized water for 15 min each to thoroughly remove residual surface contaminants. After cleaning, the samples were dried with nitrogen gas. The treated samples were then placed in a quartz tube furnace and subjected to high-temperature annealing in an atmosphere of nitrogen and hydrogen at 1 000 °C for 50 min, with the flow rate of the gas mixture maintained at 1.5 L/min throughout the process. After annealing, the samples were naturally cooled to room temperature inside the furnace, yielding porous GaN structures. To further remove any surface impurities that might have remained after annealing, the samples were ultrasonically cleaned once again and then dried with nitrogen gas for subsequent experiments.

2.2 Preparation of ZnO Nanorod/Porous GaN Heterojunctions

In this study, ZnO nanorod arrays were grown on porous p-GaN structures by a low-temperature hydrothermal method. The detailed growth procedure is described as follows: First, 2.195 g of zinc acetate dihydrate ($Zn(CH_3COO)_2·2H_2O$) was dissolved in 20 mL of 2-methoxyethanol ($CH_3OCH_2CH_2OH$), and monoethanolamine ($HOCH_2CH_2NH_2$) was added as a stabilizer to improve the uniformity and stability of the solution. The mixed solution was then continuously stirred at room temperature until a transparent and stable seed-layer solution with a concentration of 0.5 mol/L was obtained. The seed-layer solution was subsequently spin-coated onto the surface of porous p-GaN. After spin coating, the samples were placed in a quartz tube furnace and annealed at 350 °C for 60 min. Finally, the samples were vertically immersed in an autoclave containing the growth solution and subjected to hydrothermal growth at 95 °C for 3 h. The growth solution was prepared by adding $Ga(NO_3)_3$ and $Al(NO_3)_3$ solutions to a $Zn(CH_3COO)_2·2H_2O$ solution, such that the molar ratio of $Ga^{3+}/(Ga^{3+}+Al^{3+}+Zn^{2+})$ was adjusted to 1%, 3%, and 5%, respectively, while the molar ratio of $Al^{3+}/(Ga^{3+}+Al^{3+}+Zn^{2+})$ was fixed at 1%. The resulting solution was then mixed with an equal volume of hexamethylenetetramine ($C_6H_{12}N_4$) solution of the same concentration. According to the Ga dopant concentration in the growth solution from low to high, the samples were labeled S1, S2, and S3, respectively, while the undoped sample was labeled S0. After the reaction, the samples were naturally cooled to room temperature and rinsed several times with deionized water to remove residual surface reactants, thereby successfully fabricating ZnO nanorod/porous GaN heterojunctions. To investigate the electrical characteristics of the heterojunctions, indium electrodes were deposited on the surfaces of the ZnO-based nanorod arrays and GaN films by thermal evaporation. Fig. 1 schematically illustrates the fabrication process of the ZnO NRs/porous GaN heterojunction photodetector.

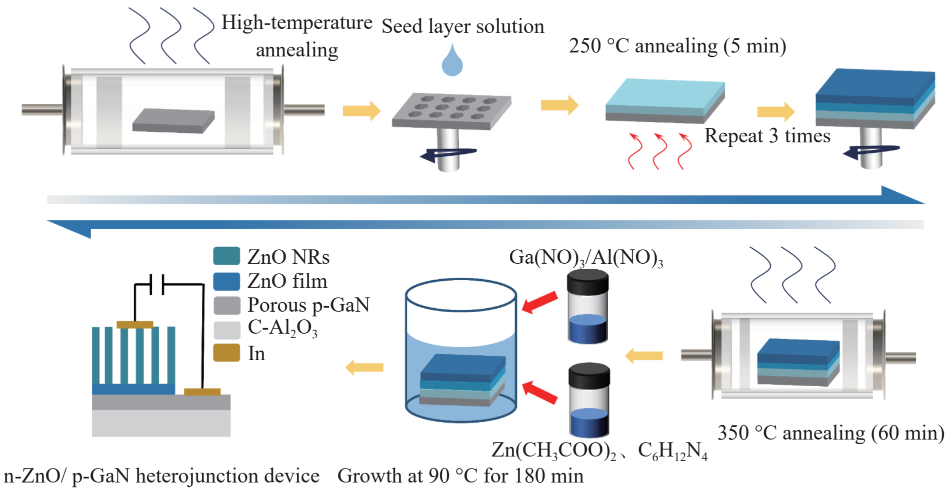

Fig. 1　Fabrication process of the ZnO NRs/porous GaN heterojunction.

2.3　Performance Characterization and Measurement

The surface morphology of the samples was characterized using a Gemini 300 scanning electron microscope (SEM, Zeiss, Germany). The optical properties of the samples were measured using a Lambda 750S UV-Vis-NIR spectrophotometer (USA). The elemental composition and chemical states of the samples were analyzed by X-ray photoelectron spectroscopy (XPS) using a Thermo Scientific Nexsa G2 system. The photoelectric performance was evaluated using a Keithley 4200-SCS semiconductor characterization system, with a 365 nm laser serving as the ultraviolet light source.

3　Results and discussion

Fig. 2a−b present the scanning electron microscopy (SEM) images of porous p-GaN. As shown in Fig. 2, uniformly distributed hexagonal pores were formed on the GaN surface after high-temperature etching, with an average pore size of approximately 183 nm and a pore density of about 2.41×10^9 cm^{-2} as statistically determined by Image J software. Fig. 2c−f show the SEM images of Ga+Al co-doped ZnO NRs/porous GaN heterojunctions with different Ga doping concentrations, directly illustrating the influence of co-doping on the morphology and growth characteristics of the nanorods. All nanorods exhibit relatively regular hexagonal top facets and grow vertically on the p-GaN surface, indicating a pronounced c-axis preferred orientation of the ZnO nanorods. Statistical analysis revealed that the average diameters of the ZnO nanorods in samples S0-S3 were 67, 54, 50, and 32 nm, respectively. With increasing Ga doping concentration, the orientational order of the Ga+Al co-doped ZnO NRs on p-GaN gradually decreased, and their average diameters became smaller than that of the undoped sample, suggesting that co-doping inhibited the radial growth of the nanorods to some extent. Meanwhile, the nanorod density showed an overall increasing trend, which may be attributed to the increase in effective nucleation sites induced by Ga+Al co-doping, thereby generating more nuclei per unit area and ultimately leading to a marked increase in nanorod density. Li *et al.*[29] found that the average diameter of ZnO nanorods decreased with increasing Ga doping concentration (0−3%). Srivastava *et al.*[30] reported that Al-doped (3 at.%) ZnO nanorods exhibited a reduced diameter and shorter length compared with undoped ZnO nanorods. Therefore, Ga and Al co-doping can effectively regulate the microscopic morphology and array structure of ZnO nanorods, thereby establishing a structural basis for further optimization of the photoelectric performance of Ga+Al co-doped ZnO NRs/porous GaN heterojunctions.

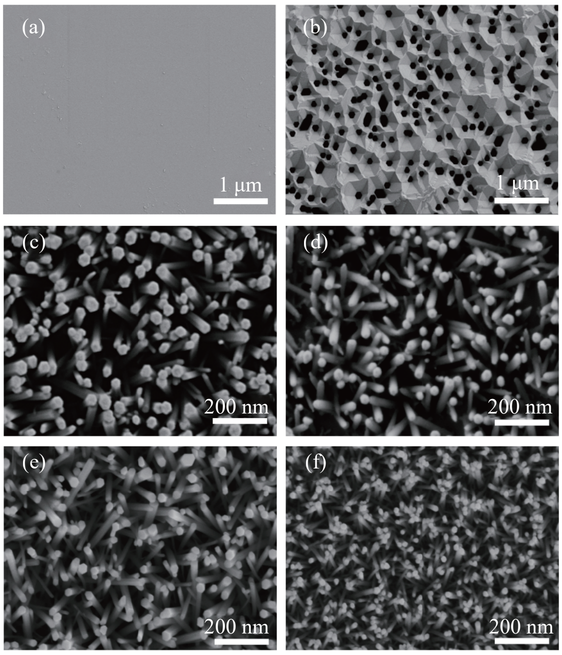

Fig. 2 SEM images of porous p-GaN films (a,b);Top-view SEM images of Ga+Al co-doped ZnO NRs/porous GaN with different Ga doping concentrations:(c) S0; (d) S1; (e) S2; and (f) S3.

Fig. 3a shows the XRD patterns of Ga+Al co-doped ZnO NRs/porous GaN heterojunctions with different Ga doping concentrations, while Fig. 3b presents an enlarged view of the (002) diffraction peak in the 2θ range of 34°−35°. All ZnO NRs/porous GaN heterojunctions exhibit a strong and sharp diffraction peak at around 2θ = 34.5°, indicating the high crystallinity of the ZnO nanorod arrays. Moreover, only the (002) and (004) diffraction peaks are observed for all heterojunctions, suggesting that the as-grown ZnO NRs are preferentially oriented along the c-axis and possess the typical hexagonal wurtzite structure. No additional diffraction peaks related to Ga- or Al-containing phases are observed, indicating the absence of secondary phases and confirming that Ga and Al were successfully incorporated into the ZnO lattice. With increasing Ga doping concentration, the (002) diffraction peak of the Ga+Al co-doped ZnO NRs shows a slight overall shift toward higher diffraction angles. This phenomenon can be attributed to the smaller ionic radii of Ga^{3+} and Al^{3+} compared with Zn^{2+}. When these ions are incorporated into the ZnO lattice and substitute for Zn sites, lattice contraction is induced, thereby causing the (002) diffraction peak to shift toward a higher angle.

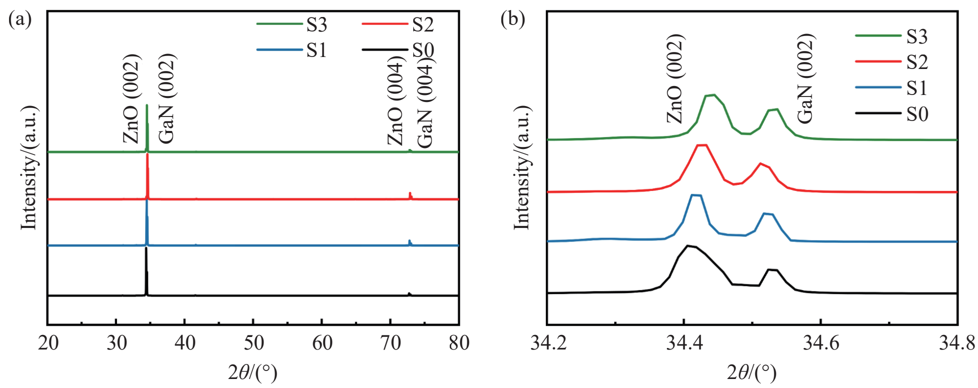

Fig. 3 XRD patterns of Ga+Al co-doped ZnO NRs/porous GaN heterojunctions with different Ga doping concentrations.

Fig. 4a shows the PL spectra of Ga+Al co-doped ZnO NRs/porous GaN heterojunctions with different Ga doping concentrations. No spectral signal originating from p-GaN was detected in any heterojunction, indicating that the incident light did not penetrate the ZnO nanorods to reach the underlying p-GaN layer and thus avoided interference from p-GaN emission during the PL measurements. All Ga+Al co-doped ZnO NRs/porous GaN heterojunctions exhibit two distinct emission features in their

PL spectra. One is a strong and sharp ultraviolet emission peak centered at approximately 379 nm, corresponding to near-band-edge (NBE) emission and generally associated with band-to-band radiative recombination or excitonic recombination in semiconductors. The other is a relatively weak broad-band emission in the visible region, extending from blue to yellow light, which is mainly attributed to defect-related radiative recombination centers such as oxygen vacancies[31]. With increasing Ga doping concentration, the intensity of the ultraviolet emission peak first increased and then decreased, reaching its maximum value for sample S2. This result indicates that the Ga+Al co-doped ZnO NRs/porous GaN heterojunction with a Ga doping concentration of 3% possessed the best crystallinity and the lowest defect density. In addition, the weak defect-related emission in the visible region further suggests that the as-prepared ZnO nanorods possess good crystallinity and excellent optical quality.

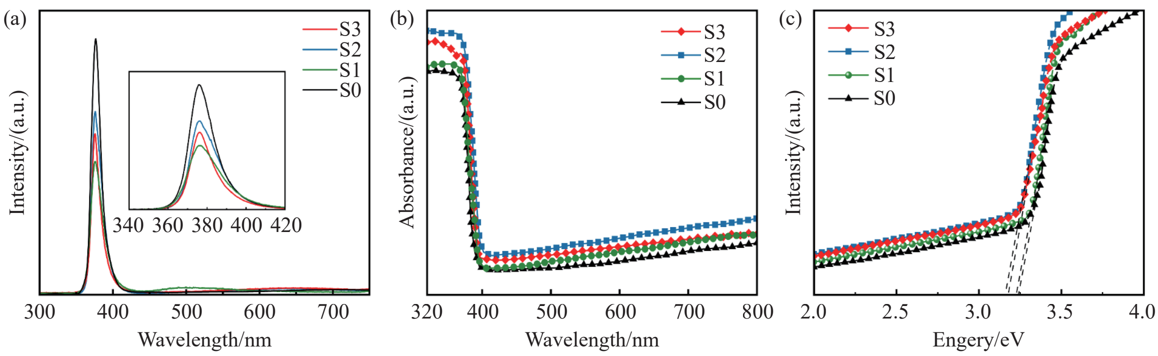

Fig. 4 (a) Photoluminescence spectra; (b) UV-visible absorption spectra; and (c) Tauc plots of Ga+Al co-doped ZnO NRs/porous GaN heterojunctions with different Ga doping concentrations.

Fig. 4b shows the UV-Vis absorption spectra of Ga+Al co-doped ZnO NRs/porous GaN heterojunctions with different Ga doping concentrations. All heterojunctions exhibit pronounced ultraviolet absorption in the wavelength range of 370-390 nm, indicating that the as-fabricated Ga+Al co-doped ZnO NRs/porous GaN heterojunctions possess strong UV-light absorption capability. This behavior is mainly attributed to the intrinsically wide bandgap of ZnO and its near-band-edge transition characteristics. In contrast, almost no obvious absorption peak is observed in the visible region, suggesting that the obtained samples exhibit excellent selective absorption in the ultraviolet range and can effectively suppress interference from visible light. According to the Tauc relation, the bandgaps of samples S0-S3 were estimated to be 3.24 eV, 3.22 eV, 3.18 eV, and 3.17 eV, respectively (Fig. 4c), which is slightly smaller than that reported for ZnO-based films prepared by the sol-gel method (3.26-3.28 eV)[32]. This slight bandgap narrowing may be related to the nanostructural characteristics of the as-prepared oxide material. With increasing Ga+Al co-doping concentration, the bandgap decreases accordingly. As the atomic ratio of Ga/Zn increases, the optical bandgap E_g decreases. This is related to factors such as the dopant concentration, impurity energy levels, and orbital hybridization of ZnO, which can alter the recombination mechanism and ultimately result in a reduction of the optical bandgap. The variation in the optical bandgap with doping concentration further indicates that the dopant species were successfully incorporated into the ZnO lattice.

To investigate the elemental composition and chemical states of the Ga+Al co-doped ZnO NRs/porous GaN heterojunctions, X-ray photoelectron spectroscopy (XPS) analysis was performed. As shown in survey spectrum (Fig. 5a), characteristic signals of Zn, O, Ga, and Al were clearly detected in the ZnO NRs/porous GaN heterojunction, confirming the presence of these elements in the fabricated heterostructure and indicating that no obvious impurity elements were introduced into the sample. The high-resolution Zn 2p spectrum of the undoped ZnO heterojunction is shown in Fig. 5b. Two characteristic peaks were observed at approximately 1 022 and 1 044 eV, corresponding to Zn $2p_{3/2}$ and Zn $2p_{1/2}$, respectively, indicating that Zn mainly existed in the ZnO lattice in the Zn^{2+} chemical state. In Fig. 5d, the peaks located at approximately 1 118 and 1 145 eV are assigned to the Ga $2p_{3/2}$ and Ga $2p_{1/2}$ electronic states, respectively. In addition, the peak located near 74 eV is attributed to the Al 2p electronic state. Fig. 5b shows that, compared with the undoped sample, the Zn 2p peak shifted slightly toward higher binding energy. Fig. 5c further shows that with increasing Ga doping concentration, the Ga 2p and Al 2p core-level peaks of the Ga+Al co-doped ZnO NRs/porous GaN heterojunctions also exhibit a slight shift toward higher binding energy. This peak shift can be attributed to changes in the average metal-oxygen bond strength induced by the incorporation of Ga and Al into the nanorods. These results indicate that doping caused a redistribution of the local electronic environment in the ZnO lattice, thereby affecting the defect states and electronic structure of the material to a certain extent. The O 1s spectra of the ZnO nanorods are shown in Fig. 5e. After peak deconvolution, the asymmetric O 1s envelope can be resolved into three components, denoted as O_I, O_{II}, and O_{III}. Among them, O_I is generally assigned to lattice oxygen (O^{2-}) in the ZnO crystal lattice; O_{II} is associated with oxygen-deficient regions and defect-related oxygen species, and is commonly regarded as being closely related to oxygen vacancies, low-coordination oxygen, or lattice distortion; O_{III} is attributed to chemically adsorbed oxygen-containing species on the surface, such as $-OH/H_2O$[33]. Notably, the Ga+Al co-doped ZnO NRs/porous GaN heterojunction with a Ga doping concentration of 3% exhibits the lowest O_{II}/O_{total} intensity ratio, indicating that the synergistic co-doping effect of Ga and Al is most pronounced at this doping level. This co-doping effect can effectively strengthen the average metal–oxygen bond strength, thereby suppressing the formation of oxygen-vacancy-related defects, reducing the defect-state density in the material, and improving its surface chemical stability. This result is also consistent with the PL measurements, in which this heterojunction exhibits the lowest visible emission intensity, indicating that co-doping can effectively suppress deep-level defects, thereby improving the optical properties and enhancing the application potential of the device.

Fig. 6 shows the current-voltage (I-V) characteristics of Ga+Al co-doped ZnO NRs/porous GaN heterojunctions with different Ga doping concentrations measured in the dark and under 365 nm ultraviolet illumination over a bias range from −3 V to +3 V, where the power density of the 365 nm light source was maintained at 0.33 mW/cm^2. As shown in Fig.6, all devices exhibit pronounced rectifying behavior, indicating the successful formation of well-defined p-n heterojunctions[34].A relatively low photocurrent-to-dark-current ratio suggests that the devices are unable to efficiently generate or separate electron-hole pairs under ultraviolet illumination, indicating that their performance still has certain limitations. In addition, a relatively high dark current limits the increase in photocurrent, thereby adversely affecting the overall device performance[35]. As illustrated in the figure., the undoped heterojunction device exhibits a relatively high dark current, with a current on/off ratio of only 81 at a bias of 3 V. In contrast, under 0 V bias and 365 nm UV illumination, sample S2 shows the most pronounced photoresponse characteristics, with a dark current as low as 0.018 nA and a photocurrent-to-dark-current ratio as high as 8.25×10^3, which further confirms its excellent optoelectronic response performance. Further comparison reveals that at both −3 V and +3 V bias, the photocurrents of the co-doped heterojunction devices are higher than those of the undoped sample, which is mainly attributed to the increased carrier concentration introduced by doping, thereby enhancing the photoresponse capability of the devices.

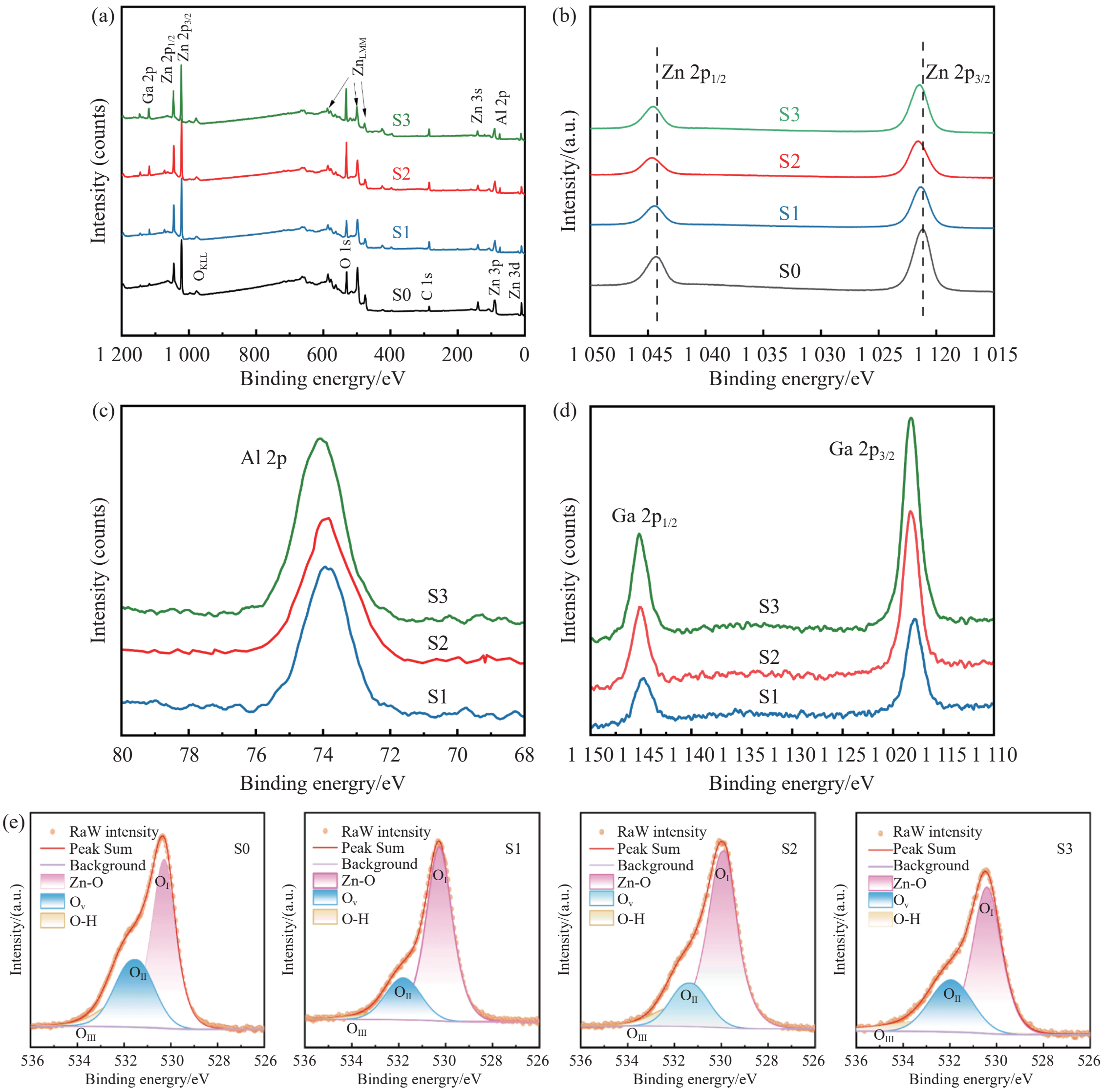

Fig. 5　XPS spectra of Ga+Al co-doped ZnO NRs/porous GaN heterojunctions with different Ga doping concentrations: (a) survey spectra; (b) Zn 2p spectra; (c) Al 2p spectra; (d) Ga 2p spectra, and (e) O1s spectra.

Responsivity (R), specific detectivity (D^*), and external quantum efficiency (EQE) are key parameters for evaluating the photodetector performance, representing the device response to incident light, photoelectric conversion efficiency, and the capability for weak-light detection. These parameters were estimated using the following equations:

$$R = (I_{photo} - I_{dark})/(PS) \quad , \qquad (1)$$

$$D^* = R/(2eJ)^{1/2} \quad , \qquad (2)$$

$$EQE = hcR/e\lambda \quad , \qquad (3)$$

where λ is the excitation wavelength, S is the effective illuminated area, e is the elementary charge, I_{dark} is the dark current, h is Planck's constant, and c is the speed of light[36-38]. The Ga+Al co-doped ZnO NRs/porous GaN heterojunction with a Ga doping concentration of 3% exhibited excellent optoelectronic performance. Under 365 nm illumination at 0 V bias, its responsivity, specific detectivity, and external quantum efficiency reached 0.158 A/W, 3.15×10^{12} Jones, and 53.5%, respectively. Compared with the device reported by Tsay *et al.*[39], the present device exhibited enhanced photocurrent and detectivity, along with improved rectification behavior. This performance enhancement is mainly attributed to the porous structure introduced into the GaN film through high-temperature etching. This structure helps relieve the stress induced by lattice mismatch and reduces the density of crystal defects. In addition, the porous structure provides a larger specific surface area, which is beneficial for the dense growth of ZnO nanorods and the strengthening of interfacial bonding, thereby increasing the effective interfacial contact area. Such a three-dimensional heterostructure further promotes the separation and transport efficiency of photogenerated carriers.

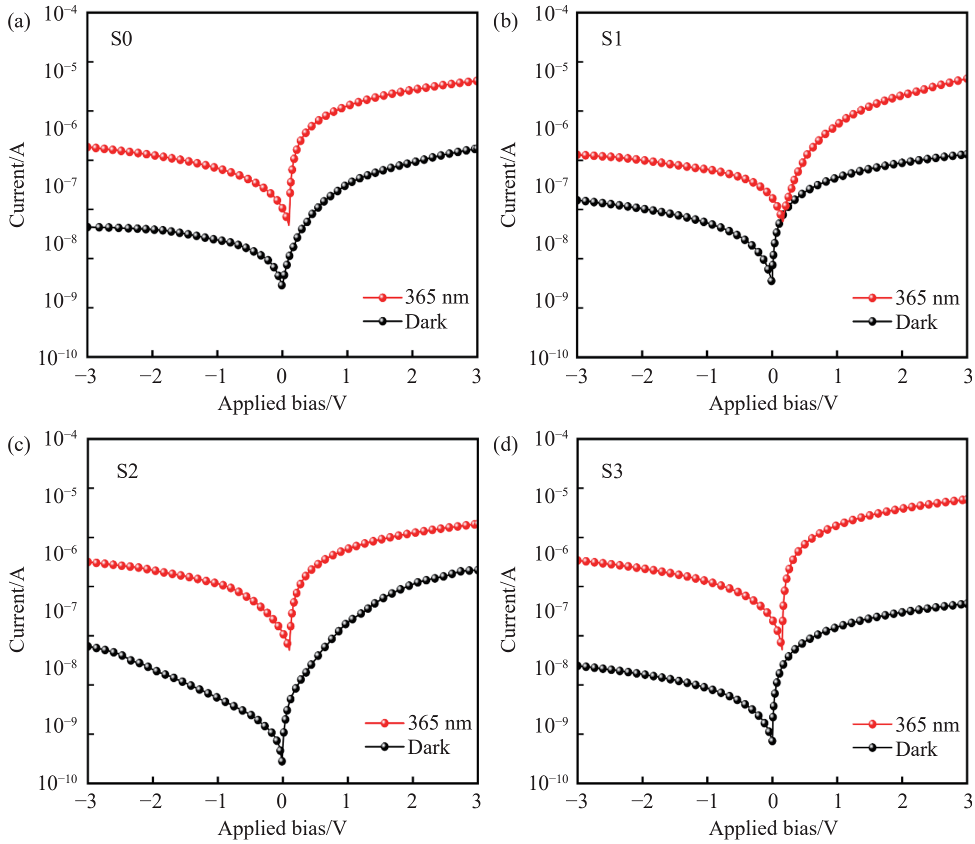

Fig. 6 I-V characteristics of Ga+Al co-doped ZnO NRs/porous GaN heterojunctions with different Ga doping concentrations: (a)S0; (b)S1; (c)S2; (d)S3.

Table 1 compares the performance of the present heterojunction photodetector with that of other reported ZnO/GaN-based photodetectors at 0 V bias. Compared with previously reported devices, the ZnO nanorod/porous GaN heterojunction fabricated by the low-temperature hydrothermal method exhibits a lower dark current as well as higher external quantum efficiency and specific detectivity, indicating that this device combines low-noise characteristics with excellent sensitivity for weak-light detection. As a result, it can effectively identify and stably detect weak ultraviolet signals, demonstrating promising UV photodetection performance and considerable application potential.

Tab. 1 Performance comparison of the ZnO NRs/porous GaN heterojunction photodetector (sample S2) and other reported ZnO/GaN based photodetectors under 0 V bias.

Photodetector	λ (nm)	R (mA/W)	D* (Jones)	EQE (%)	Reference
P-GaN/n-ZnO film	368	11	6.2×10^{11}	3.71	[22]
P-GaN/n-ZnO NRs	365	138.9	10^{12}	47.6	[39]

续表 1

Photodetector	λ (nm)	R (mA/W)	D* (Jones)	EQE (%)	Reference
P-GaN/n-ZnO microwire	370	137	2.15×10^{12}	45.9	[3]
P-GaN/n-ZnO:Ga NRs	365	230	2.32×10^{12}		[40]
P-GaN/n-ZnO: In+La film	366	46	9.92×10^{11}	15.6	[26]
P-GaN/n-ZnO:Ga+In NRs		5.29	7.98×10^{9}	1.79	[27]
Porous p-GaN/n-ZnO:Ga+Al NRs	365	158	3.15×10^{12}	53.5	This work

Stability and response speed are key parameters for evaluating photodetection performance.As shown in Fig. 7, the I-t characteristics of Ga+Al co-doped ZnO NRs/porous GaN heterojunction ultraviolet photodetectors with different Ga doping concentrations were measured under 365 nm illumination at 0 V bias with a cycle of 10 s, and stable photocurrent responses were obtained. All four p-n heterojunctions exhibited stable and reproducible photoresponse behavior during repeated on/off cycling tests, indicating that the devices possessed good cyclic stability and reliability and could satisfy the requirements for long-term operation in practical applications. Owing to their photovoltaic characteristics, ultraviolet photodetectors based on p-n junction structures are capable of detecting UV signals under zero-bias conditions. Upon UV illumination, the device current rapidly reached its peak value, followed by a slight decrease and then stabilized at a relatively constant level. When the illumination was turned off, the photocurrent decreased rapidly and gradually returned to its initial dark-current state, showing a typical reversible transient response. Among them, the S2 device exhibited the best response kinetics, with a rise time and a decay time of 0.13 and 0.21 s, respectively, which were clearly superior to those of the other samples, namely S0 (0.18/0.26 s), S1 (0.20/0.31 s), and S3 (0.23/0.30 s). These results indicated that the Ga+Al co-doped ZnO NRs/porous GaN heterojunction device with a Ga doping concentration of 3% exhibited the best transient photoresponse performance, with relatively short rise and decay times, suggesting that the synergistic modulating effect of Ga and Al is most pronounced at this doping level. An appropriate Ga doping concentration not only helped improve the crystallinity and carrier transport properties of ZnO nanorods, but also effectively reduced the trapping of photogenerated carriers by defect-related trap states, thereby accelerating the separation, transport, and recombination recovery processes of photogenerated carriers and ultimately enabling a faster response rate and better dynamic photodetection performance.

The photoresponse mechanism of the ZnO/GaN heterojunction photodetector can be explained by its energy band structure, as illustrated in Fig. 7(c). In this figure, E_C, E_V, and E_F represent the conduction band minimum, valence band maximum, and Fermi energy level of the material, respectively. The wide bandgaps of GaN and ZnO (Eg > 3.3 eV) make them highly suitable for ultraviolet photodetection. When a p-GaN/n-ZnO heterojunction is formed, band bending at the interface generates a built-in electric field, which enables rapid separation and efficient collection of photogenerated carriers under zero bias while suppressing recombination in the junction region, thereby achieving a significant photoresponse. Under ultraviolet illumination, when the photon energy exceeds the semiconductor bandgap, photogenerated electron–hole pairs can be excited. Subsequently, driven by the built-in electric field, photogenerated electrons drift toward the n-ZnO side (from the p-GaN side into n-ZnO), while photogenerated holes drift toward the p-GaN side (from the n-ZnO side into p-GaN). Under zero bias, the built-in electric field in the depletion region of the p-GaN/n-ZnO heterojunction drives the rapid separation and directional transport of photo-generated carriers, thereby producing a measurable photocurrent (photovoltaic response).

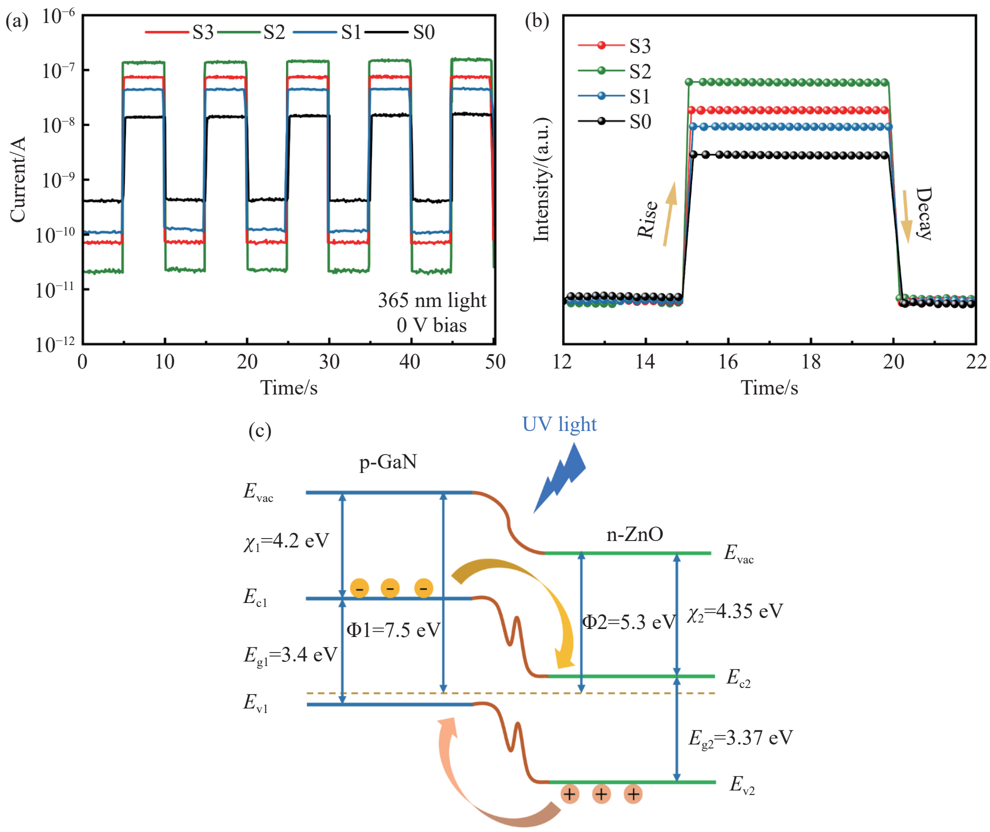

Fig. 7 (a) I-t characteristic curves and (b) time response curves of Ga+Al co-doped ZnO NRs/porous GaN heterojunctions with different Ga doping concentrations under zero bias and 365 nm illumination; (c) Energy band diagrams of ZnO/GaN heterojunction.

4 Conclusions

In this work, Ga+Al co-doped ZnO nanorod arrays with different Ga doping concentrations were grown on porous p-GaN films via a low-temperature hydrothermal method, and ZnO/GaN-based heterojunction ultraviolet photodetectors were successfully fabricated. SEM results showed that the average diameter of the undoped ZnO nanorod array was 67 nm. When the Al doping concentration was fixed at 1% and the Ga doping concentration was set at 1%, 3%, and 5%, the average diameters of the ZnO nanorod arrays were 54, 50, and 32 nm, respectively. With increasing Ga doping concentration, the orientational ordering of the Ga+Al co-doped ZnO NRs on p-GaN decreased, and their average diameters became smaller than that of the undoped sample, indicating that co-doping exerts an inhibitory effect on the radial growth of the nanorods. In addition, Ga+Al co-doping increases the density of effective nucleation sites in the solution, leading to the formation of more nuclei per unit area and consequently a significant increase in nanorod density. XRD results indicated that all heterojunctions exhibited preferential c-axis-oriented growth on the porous p-GaN films. XPS further confirmed the presence and corresponding chemical states of the dopant elements (Ga and Al), indicating that the dopants were successfully incorporated into the ZnO nanorods. The I-V characteristics revealed that the Ga+Al co-doped ZnO NRs/porous GaN heterojunction with a Ga doping concentration of 3% exhibited a dark current of 0.018 nA and, under 365 nm illumination, achieved a light/dark current ratio of 8 250, a responsivity of 158 mA/W, and a specific detectivity of 3.15×10^{12} Jones. These results demonstrate that heterojunctions constructed from porous GaN structures and ZnO-based nanostructures are promising candidates for high-performance ultraviolet photodetection applications.

Conflicts of interest

The authors declare no conflict of interest.

References:

[1] LIN·H W, JIANG·A, XING·SH B, *et al*.. Advances in self-powered ultraviolet photodetectors based on P-N heterojunction low-dimensional nanostructures[J]. *Nanomaterials*, 2022, 12(6): 910.

[2] HOU·X H, ZHAO·X L, ZHANG·Y, *et al*.. High-performance harsh-environment-resistant GaO_x solar-blind photodetectors via defect and doping engineering[J]. *Advanced Materials*, 2022, 34: 2106923.

[3] XIE·Y L, WAN·P, JIANG·M M, *et al*.. Performance enhancement of a self-biased n-ZnO microwire/p-GaN heterojunction ultraviolet photodetector incorporating Ag nanowires[J]. *CrystEngComm*, 2022, 24: 7727-7738.

[4] CAO·F, LIU·Y, LIU·M, *et al*.. Wide bandgap semiconductors for ultraviolet photodetectors: approaches, applications, and prospects[J]. *Research*, 2024, 7: 0385.

[5] XIAO·Y, LIU·L, MA·ZH·H, *et al*.. High-performance self-powered ultraviolet photodetector based on Nano-porous GaN and CoPc *p-n* vertical heterojunction[J]. *Nanomaterials*, 2019, 9(9): 1198.

[6] JIA·K D, JIA·W, LI·T B, *et al*.. Fabrication of porous $CuxZn_{1-x}S$/GaN heterojunctions for ultraviolet photodetector application[J]. *Optical Materials*, 2025, 162: 116881.

[7] WEN·J J, WANG·Y K, ZHANG·B, *et al*.. High-performance ultraviolet photodetectors based on nanoporous GaN with a Ga_2O_3 single-crystal layer[J]. *Nanomaterials*, 2024, 14(13): 1165.

[8] CUI·J SH, ZHOU·J P, CHEN·H M, *et al*.. Effect of ultraviolet and room lights on porous GaN films using photo-assisted electrochemical etching[J]. *Materials Letters*, 2021, 301: 130287.

[9] CHEN·C·H, CHANG·S·J, SU·Y·K, *et al*.. Vertical high quality mirrorlike facet of GaN-based device by reactive ion etching[J]. *Japanese Journal of Applied Physics*, 2001, 40: 2762-2764.

[10] ZHANG·L, WANG·SH ZH, SHAO·Y L, *et al*.. One-step fabrication of porous GaN crystal membrane and its application in energy storage[J]. *Scientific Reports*, 2017, 7: 44063.

[11] CHEN·R R, LIU·J, FENG·B, *et al*.. Pores in p-type GaN by annealing under nitrogen atmosphere: formation and photodetector[J]. *Journal of Materials Science*, 2022, 57(1): 467-476.

[12] MENG R L, JI·X L, LOU·ZH, *et al*.. High-performance nanoporous-GaN metal-insulator-semiconductor ultraviolet photodetectors with a thermal oxidized β-Ga_2O_3 layer[J]. *Optics Letters*, 2019, 44(9): 2197-2200.

[13] YU·R X, WANG·G D, SHAO·Y L, *et al*.. From bulk to porous GaN crystal: precise structural control and its application in ultraviolet photodetectors[J]. *Journal of Materials Chemistry C*, 2019, 7(45): 14116-14122.

[14] PU·T F, YOUNIS·U, CHIU·H·C, *et al*.. Review of recent progress on vertical GaN-based PN diodes[J]. *Nanoscale Research Letters*, 2021, 16: 101.

[15] NOMOTO·K, SONG·B, HU·Z Y, *et al*.. 1.7-kV and 0.55 mΩ·cm2 GaN p-n diodes on bulk GaN substrates with avalanche capability[J]. *IEEE Electron Device Letters*, 2016, 37(2): 161-164.

[16] 郭越, 孙一鸣, 宋伟东. 多孔 GaN/CuZnS 异质结窄带近紫外光电探测器[J]. 物理学报, 2022, 71(21): 218501.
GUO·Y, SUN·Y·M, SONG·W·D. Narrowband near-ultraviolet photodetector fabricated from porous GaN/CuZnS heterojunction[J]. *Acta Physica Sinica*, 2022, 71(21): 218501.

[17] VARSHNEY·U, SHARMA·A, VASHISHTHA·P, *et al*.. Ga_2O_3/GaN heterointerface-based self-driven broad-band ultraviolet photodetectors with high responsivity[J]. *ACS Applied Electronic Materials*, 2022, 4(11): 5641-5651.

[18] ZHANG·J T, TANG·K, WEI·T CH, *et al*.. High-photosensitive ultraviolet photodetector based on an *n*-ZnO microwire/p-InGaN heterojunction[J]. *Physica E: Low-dimensional Systems and Nanostructures*, 2023, 146: 115562.

[19] JIN·Y M, JIAO·SH, WANG·D B, *et al*.. Enhanced UV photoresponsivity of ZnO nanorods decorated with Ag_2S/ZnS nanoparticles by successive ionic layer adsorption and reaction method[J]. *Nanomaterials*, 2021, 11(2): 461.

[20] BAKRY·M, ISMAIL·W, ABDELFATAH·M, *et al*.. Low-cost fabrication methods of ZnO nanorods and their physical and photoelectrochemical properties for optoelectronic applications[J]. *Scientific Reports*, 2024, 14: 23788.

[21] HONG·S·K, KO·H·J, CHEN·Y F, *et al*.. Defect characterization in epitaxial ZnO/epi-GaN/Al_2O_3 heterostructures: transmission electron microscopy and triple-axis X-ray diffractometry[J]. *Journal of Crystal Growth*, 2000, 209(2-3): 537-541.

[22] KAUR·A, ARORA·S, CHETRY·P, *et al*.. (0001)n-ZnO/(0001)p-GaN heterostructure based self-driven fast UV photodetectors and the role of the polarization induced interfacial 2D electron gas channel[J]. *ACS Applied Electronic Materials*, 2024, 6(9): 6619-6625.

[23] FAN·ZH H, KUAI·Y, XU·Y T, *et al*.. Self-assembly ZnO mesh and GaN heterojunction voltage sensitive ultraviolet photodetector[J]. *Materials Today Communication*, 2025, 42: 111452.

[24] CABRAL·L, LOPEZ RICHARD·V, DA SILVA·J·L·F, *et al*.. Insights into the nature of optically active defects of ZnO[J]. *Journal of Luminescence*, 2020, 227: 117536.

[25] YOUNG·S·J, YANG·C·C, LAI·L·T. Review-growth of Al-, Ga-, and In-doped ZnO nanostructures via a low-temperature process and their application to field emission devices and ultraviolet photosensors[J]. *Journal of the Electrochemical Society*, 2017, 164(5): B3013-B3028.

[26] DING·H R, PENG·Y, CHEN·M Q, *et al*.. Improved detection performance of self-driven InZnO/p-GaN heterojunction UV photodetector by lanthanum doping[J]. *Journal of Alloys and Compounds*, 2023, 966: 171537.

[27] TSAY·C·Y, HSIAO·I·P, CHANG·F·Y, *et al*.. Improving the photoelectrical characteristics of self-powered p-GaN film/n-ZnO nanowires heterojunction ultraviolet photodetectors through gallium and indium co-doping[J]. *Materials Science in Semiconductor Processing*, 2021, 121: 105295.

[28] LUNG·C, TOMA·M, POP·M, *et al*.. Characterization of the structural and optical properties of ZnO thin films doped with Ga, Al and (Al+Ga)[J]. *Journal of Alloys and Compounds*, 2017, 725: 1238-1243.

[29] LI·R, YU·CH Y, DONG·H L, *et al*.. Effects of $Ga_xZn_{1-x}O$ nanorods on the photoelectric properties of n-ZnO nanorods/p-GaN heterojunction light-emitting diodes[J]. *RSC Advances*, 2017, 7(78): 49613-49617.

[30] SRIVASTAVA·V, BABU·E·S, HONG·S·K. Effect of Al doping on the properties of ZnO nanorods synthesized by hydrothermal growth for gas sensor applications[J]. *Korean Journal of Materials Research*, 2020, 30(8): 399-405.

[31] ALNAIM·N, KUMAR·S, ALSHOAIBI·A. Structural, morphological, electronic structural, optical, and magnetic properties of ZnO nanostructures[J]. *Materials*, 2022, 15(24): 8889.

[32] TSAY·C·Y, LEE·W·C. Effect of dopants on the structural, optical and electrical properties of sol-gel derived ZnO semiconductor thin films[J]. *Current Applied Physics*, 2013, 13(1): 60-65.

[33] CHANG·F·M, BRAHMA·S, HUANG·J·H, *et al*.. Strong correlation between optical properties and mechanism in deficiency of normalized self-assembly ZnO nanorods[J]. *Scientific Reports*, 2019, 9: 905.

[34] JIA·W, REN·H L, LI·T B, *et al*.. Fabrication of porous Ga_2O_3/GaN heterojunction for ultraviolet photodetector application[J]. *Optics Express*, 2025, 33(9): 18993-19003.

[35] LV·Z X, YAN·SH Q, MU·W X, *et al*.. A high responsivity and photosensitivity self-powered UV photodetector constructed by the CuZnS/Ga_2O_3 heterojunction[J]. *Advanced Materials Interfaces*, 2023, 10(5): 2202130.

[36] LI·SH, ZHI·Y S, LU·CH, *et al*.. Broadband ultraviolet self-powered photodetector constructed on exfoliated β-Ga_2O_3/CuI core-shell microwire heterojunction with superior reliability[J]. *The Journal of Physical Chemistry Letters*, 2021, 12(1): 447-453.

[37] LI·SH, YUE·J Y, JI·X Q, *et al*.. Oxygen vacancies modulating the photodetector performances in ε-Ga_2O_3 thin films[J]. *J. Mater. Chem. C*, 2021, 9(16): 5437-5444.

[38] LI·SH, YUE·J Y, YAN·Z Y, *et al*.. Enhancing the self-powered performance in VO_x/Ga_2O_3 heterojunction ultraviolet photodetector by hole-transport engineering[J]. *Journal of Alloys and Compounds*, 2022, 902: 163801.

[39] MISHRA·M, GUNDIMEDA·A, GARG·T, *et al*.. ZnO/GaN heterojunction based self-powered photodetectors: influence of interfacial states on UV sensing[J]. *Applied Surface Science*, 2019, 478: 1081-1089.

[40] YANG·L, ZHOU·H, XUE·M N, *et al*.. A self-powered, visible-blind ultraviolet photodetector based on n-Ga: ZnO nanorods/p-GaN heterojunction[J]. *Sensors and Actuators A: Physical*, 2017, 267: 76-81.

Author Biographies：

YANG Xudong (2001—), male, born in Changzhi, Shanxi Province, master's student. He received his bachelor's degree from Taiyuan University of Science and Technology in 2023. His research mainly focuses on optoelectronic materials and devices. E-mail: yyyxudong@163.com

JIA Wei (1983—), male, born in Yuncheng, Shanxi Province, Ph.D., Senior Technician, Master's Supervisor, received his Ph.D. degree from Taiyuan University of Technology in 2013. His main research focuses on semiconductor optoelectronic materials and devices. E-mail: jiawei@tyut.edu.cn